

Short Communication

Thin foil transformation into liquid droplets due to the Rayleigh–Taylor instability in NDCX-1 experiments[☆]

Igor D. Kaganovich*, Edward A. Startsev, Ronald C. Davidson

Plasma Physics Laboratory, Princeton University, Princeton, NJ 08543, United States

ARTICLE INFO

Article history:

Received 2 May 2011

Received in revised form

28 June 2011

Accepted 28 June 2011

Available online 7 July 2011

Keywords:

Liquid droplets

Rayleigh–Taylor instability

NDCX-1 experiment

ABSTRACT

It is proposed that a likely scenario for droplet formation in the NDCX-I experiments is a result of the Rayleigh–Taylor instability for targets with a thickness larger than the range of ions in the film (~100 nm for NDCX-I parameters).

© 2011 Elsevier B.V. All rights reserved.

In experiments on the neutralized drift current experiment (NDCX-I) facility an intense ion beam heat a thin foil above the melting temperature. For NDCX-I parameters the thin film is liquefied, but it is not evaporated completely into a gas. Instead, the liquefied foil is dissembled into droplets. A possible mechanism of droplet formation is the Rayleigh–Taylor instability associated with the liquid film acceleration due to a small difference of vapor pressures at the front and back sides of the film. Both sides of the foil evaporate, but at slightly different rates. This imbalance in vapor pressure produces a net acceleration of the thin liquid film toward one side, and the Rayleigh–Taylor instability develops as a result of this acceleration. The perpendicular size of the perturbations is determined by the maximum growth rate of the Rayleigh–Taylor instability as a function of the perturbation size, and is affected by the surface tension. Droplets are then formed during the nonlinear stage of the instability.

In the neutralized drift current experiment (NDCX-I) a thin target foil is heated by an ion beam pulse to temperatures above the melting point [1]. After the target is heated above the melting point, the target is observed to disassemble into droplets [2], as shown in Fig. 1. There could be several mechanisms for droplet formation.

- Destruction of the solid film due to a build-up of tension before the film is liquefied.

- Formation of the droplet from the evaporated gas during expansion into vacuum, and subsequent cooling [3].
- Formation of droplets due to the Marangoni effect. The large gradients of temperature along the film surface cause an inhomogeneous surface tension due to its dependence on temperature. Such a force results in liquid stratification and droplet formation [2].
- For films with thickness larger than the range of ions in the film, the Rayleigh–Taylor instability could be a result of acceleration of the liquefied film due to a difference of vapor pressures at the front and back sides of the film.

Estimates show that for the intensity of the ion beam in the NDCX-I experiment, a thin foil is liquefied by the intense ion beam pulse, but it is not transformed into a gas [4]. Therefore, in the NDCX-I experiment, the droplets are not formed from the evaporated gas during expansion into vacuum. The Marangoni effect was discussed in Ref. [2]. In the following we consider only the last effect. We will show that the Rayleigh–Taylor instability may be responsible for the observed formation of submicron droplets during several microseconds of liquefied film expansion into vacuum. Reference [2] shows that the Marangoni effect can give time scales and spatial scales for droplet formation similar to the Rayleigh–Taylor instability. Further delineation between the two effects and a study of possible target breakup can be performed by making use of a 3D fluid code, which incorporates a model for the surface tension and material spall. Such a code is currently under development [5].

[☆] Research supported by the U.S. Department of Energy.

* Corresponding author.

E-mail address: ikaganov@pppl.gov (I.D. Kaganovich).

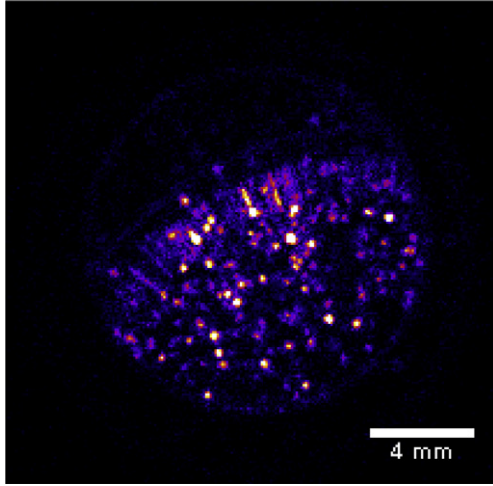


Fig. 1. Beam irradiation of Pt foil led to images of what appears to be droplets and scattered light up to 500 μ s after the beam pulse passes through the target film on NDCX-I [1,2]. This image is the self-emission downstream from a 120 nm Pt target; the image is taken by a Princeton Instruments PIMAX camera with 5 μ s gate.

Both sides of the liquefied film evaporate into a vacuum, but at slightly different rates. This imbalance in vapor pressure produces a net acceleration of the thin liquid film toward one side, and the Rayleigh-Taylor instability develops as a result of this acceleration. The perpendicular size of the perturbations is determined by the maximum growth rate as a function of the perturbation size, and is affected by the surface tension. Droplets are then formed during the nonlinear stage of the instability.

In the present analysis, we make use of the Van der Waals equation-of-state (EOS), i.e.,

$$(P + n^2 a)(1 - nb) = nRT,$$

where, P is the pressure, n is the density, $R = kN_A$ is the gas constant. The constant a is a measure for the attraction between the particles, and the constant b is the volume excluded by a particle [6]. For this equation-of-state, the attraction energy of one atom to another atom at the minimum of the pair interaction potential is related to the temperature at the critical point, i.e., $\varepsilon = 81T_{cr}/32$ for a Lennard-Jones potential [7], where quantities are expressed in eV. The pressure of the evaporated gas is given by the Clausius–Clapeyron relation [8], i.e.,

$$P_{vap} = 27P_{cr} \exp\left(-\frac{27}{8} \frac{T_{cr}}{T}\right). \quad (1)$$

Here, P_{cr} is the pressure at the critical point. For the Van der Waals equation-of-state, P_{cr} is given by [9]

$$P_{cr} = 3n_{cr}T_{cr}/8. \quad (2)$$

The density of a liquid corresponds to the point where the pressure is nearly zero (equilibrium), which gives $n \equiv n_{\bar{n}} \approx 3n_{cr}$ ($n_{\bar{n}} \approx 1/b = 3n_{cr}$).

The film temperature can be determined from the balance between the power of the long pre-pulse (I) and heat removal through the evaporation process according to the relation [6]

$$I = 2\varepsilon \Gamma_{vap} = 2\varepsilon \frac{P_{vap}}{\sqrt{2\pi m T}}. \quad (3)$$

Substituting Eq. (1) into Eq. (3) gives

$$I = \frac{3}{2} \left(\frac{27}{8}\right)^2 \frac{n_{\bar{n}} T_{cr}^2}{\sqrt{2\pi m T}} \exp\left(-\frac{27}{8} \frac{T_{cr}}{T}\right). \quad (4)$$

Eq. (4) allows a determination of the temperature established in the liquefied film at a given beam power. For example, for gold, $n_{\bar{n}} m = 17 \text{ g/cm}^3$, $T_{cr} = 7500 \text{ K}$, and $m = 197m_p$, where m is the atom mass, and m_p is the proton mass. And if a gold film reaches a temperature $0.4T_{cr} = 3000 \text{ K}$, the beam power is about 500 kW/cm^2 , corresponding to the typical energy density in a focused NDCX-1 beam [2]. The minimum heating time required for the film to reach this temperature is determined by the heat capacity of the metal, which is $C_p = 3 \text{ k}$. This gives $\Delta t > n\Delta x C_p T$, where Δx is the width of the film, and Δt is the minimum time it takes to heat the sample. For a $1 \mu\text{m}$ film, this gives a minimum time of $1 \mu\text{s}$ for heating the foil up to 3000 K .

The difference in temperatures on both sides of the foil can be estimated by making use of the heat conduction equation,

$$\frac{d^2}{dx^2} \chi T = \frac{dl}{dx},$$

where dl/dx is the energy deposited into the volume by the beam stopping power, and χ is the heat conductivity. For example, for gold, $\chi = 310 \text{ W/m K}$ [10]. The maximum difference in temperatures between the two sides corresponds to the limit where the beam penetration depth is small compared with the film thickness. For the 300 keV potassium beam in NDCX-I, the range of the beam ions in gold is 90 nm [11].

For NDCX-I parameters, the temperature difference is small due to the fact that the heat conduction is high. The deposited beam power is transported to both sides of the foil quickly by heat conduction, and is balanced by evaporation. Because the temperature in the foil is nearly uniform, and the vapor flux is a function of temperature given by Eq. (1), approximately one-half of the power is conducted to one side of the foil and one-half to the other. Therefore, at the edges, $x = \pm \Delta x/2$, we obtain $(d/dx)\chi T|_{x=\pm \Delta x/2} = I/2$. If the penetration depth is small compared with the film thickness, then $\chi \Delta T = 1/2 I \Delta x$, or equivalently,

$$\chi \Delta T|_{x=\pm \Delta x/2} = \varepsilon \frac{27P_{cr} \exp\left(-\frac{27}{8} \frac{T_{cr}}{T}\right)}{\sqrt{2\pi m T}} \Delta x. \quad (5)$$

For a $1 \mu\text{m}$ gold film heated by intense beam with power density $I = 500 \text{ kW/cm}^2$, the calculation making use of Eq. (5) then gives the estimate

$$\frac{\Delta T_{max}}{T} \sim 2.8 \times 10^{-3}.$$

Substituting Eq. (5) into Eq. (1) shows that the pressure difference between the two sides is given by

$$\frac{\Delta P_{vap}}{P_{vap}} = \frac{27}{8} \frac{T_{cr}}{T} \frac{\Delta T}{T},$$

and is of order 2.4×10^{-2} .

The acceleration of the film as a whole is given by [12]

$$g = \frac{\Delta P_{vap}}{\rho \Delta x}. \quad (6)$$

Substituting the pressure and film thickness, $1 \mu\text{m}$, gives $g = 5.7 \times 10^6 \text{ m/s}^2$ or $5.7 \mu\text{m}/(\mu\text{s})^2$. Such a value of acceleration is fast enough to significantly distort the film on a μs time scale. Calculation of the maximum growth rate of the Rayleigh-Taylor instability for the thin film accelerated toward one side gives

$$\gamma \approx \sqrt{\frac{g \Delta x}{2a_c^2}}, \quad (7)$$

where $a_c = \sqrt{\alpha/\rho g}$ is the capillary length, if $\Delta x < a_c$. In the opposite limit, $\Delta x > a_c$, it follows that [13]

$$\gamma = \sqrt{\frac{2g}{3^{3/2}a_c}}.$$

Here, $\alpha = Cp_{cr}^{2/3}T_{cr}^{1/3}(1 - T/T_{cr})$ is the surface tension given by the Guggenheim–Katayama relation [6]. Typically, the Eötvös law can also be used to obtain the value of the surface tension $(d/dT)[\alpha(\rho/M)^{-2/3}] = -2.12$, where α is given in milli-N/m, ρ is in g/cm^3 , T is the temperature in K [14] and $\alpha(T_{cr}) = 0$. However, application of the Eötvös law to gold gives $\alpha = 2.5$ N/m at 1338 K, instead of the tabulated value of $\alpha = 1.145$ N/m [14]. Therefore, the coefficient -2.12 has been reduced to -1 . Then, the Eötvös law gives $\alpha = 0.87$ N/m at $T = 3000$ K and $a_c = 2.6$ μm . Finally, Eq. (7) gives for the estimate of the growth rate of the Rayleigh–Taylor instability

$$\gamma \approx 0.6 \mu\text{s}^{-1} \quad (8)$$

for a $\Delta x = 1$ μm film and $a_c \sim 2.6$ μm . Therefore, target can disassemble into droplets on time scale of few microseconds corresponding to development of the nonlinear stage of the Rayleigh–Taylor instability.

In summary, it is proposed that a likely scenario for droplet formation in the NDCX-I experiments is a result of the Rayleigh–Taylor instability for targets with a thickness larger than the range of ions in the film (~ 100 nm for NDCX-I parameters).

References

- [1] F.M. Bieniosek, E. Henestroza, S. Lidia, P.A. Ni, Review of Scientific Instruments 81 (2010) 10E112;
- [2] F.M. Bieniosek, J.J. Barnard, E. Henestroza, B.G. Logan, S. Lidia, R.M. More, P.A. Ni, P.A. Seidl, Measure and Simulate Target Temperature and Dynamic Response in Optimized NDCX-I Configurations with Initial Diagnostics Suite," 4th Quarter 2009 Milestone Report Heavy Ion Fusion. Science Virtual National Laboratory 4th quarter, September 30, 2009, LBNL-3038E.
- [3] B. Chimier, V.T. Tikhonchuk, Phys. Rev. B. 79 (2009) 184107.
- [4] P.A. Ni, F.M. Bieniosek, M. Leitner, C. Weber, W.L. Waldron, Nuclear Instruments and Methods in Physics Research A 606 (2009) 169–171.
- [5] Alice Koniges, et al., ALE – AMR-Arbitrary Lagrangian Eulerian Adaptive Mesh Refinement ALE-AMR Code. <http://www.nersc.gov/assets/HPC-Requirements-for-Science/Friedman-FES-2010.pdf>, 2011.
- [6] L.D. Landau, E.M. Lifshitz, Statistical Physics, third ed., Vol. 5, Butterworth-Heinemann, Oxford, 1980.
- [7] J.E. Lennard-Jones, On the determination of Molecular Fields, Proceedings of the Royal Society Series A 106 (738) (1924) 463–477.
- [8] Kenneth Wark, Generalized Thermodynamic Relationships, Thermodynamics, fifth ed. McGraw-Hill, Inc., New York, NY, 1988.
- [9] V.E. Fortov, I.T. Yakubov, The Physics of Non-Ideal Plasma. World Scientific, 2000, Appendix 1.
- [10] www.engineeringtoolbox.com/thermal-conductivity-d_429.html.
- [11] SRIM data. www.srim.org, 2011.
- [12] Here, we neglected momentum of the beam pulse transferred to the film compared with momentum transferred due to difference of gas pressure at opposite sides. Indeed, energy of a 300 KeV beam ion is sufficient to evaporate millions of vapor particles, which have momentum 1000 times more than the one 300 keV ion. Therefore, even few percent differences in pressure at opposite sides yields momentum transferred to the film large compared with the momentum of the beam pulse.
- [13] L.D. Landau, E.M. Lifshitz, Fluid Mechanics, , In: Course of Theoretical Physics, second ed., Vol. 6, Butterworth-Heinemann, Oxford, 1987.
- [14] www.kayelaby.npl.co.uk/general_physics/2_2/2_2_5.html.